

## Supplementary Information

### **PVP-stabilized cerium oxide-platinum nanocomposite synthesized in TEG: pro-/antioxidant activities**

Nadiia M. Zholobak<sup>1,2\*</sup>, Iryna V. Dubova<sup>1</sup>, Anastasiia Deineko<sup>3</sup>, Viacheslav Kalinovych<sup>3</sup>, Jaroslava Nováková<sup>3</sup>, Iva Matolínová<sup>3</sup>, Kevin C. Prince<sup>3,4</sup>, Tomáš Skála<sup>3</sup>, Alexander B. Shcherbakov<sup>1</sup>, Nataliya Tsud<sup>3</sup>

<sup>1</sup> Zabolotny Institute of Microbiology and Virology, National Academy of Sciences of Ukraine, Zabolotny Street 154, Kyiv, 03680, Ukraine

<sup>2</sup> Kyiv National University of Technologies and Design, Mala Shyianovska Street 2, Kyiv, 01011, Ukraine

<sup>3</sup> Charles University, Faculty of Mathematics and Physics, Department of Surface and Plasma Science, V Holešovičkách 2, Prague, 18000, Czech Republic

<sup>4</sup> Elettra-Sincrotrone Trieste S.C.p.A., in Area Science Park, Strada Statale 14 km 163.5, Basovizza (Trieste), 34149, Italy

\* Corresponding author e-mail address: n.zholobak@gmail.com

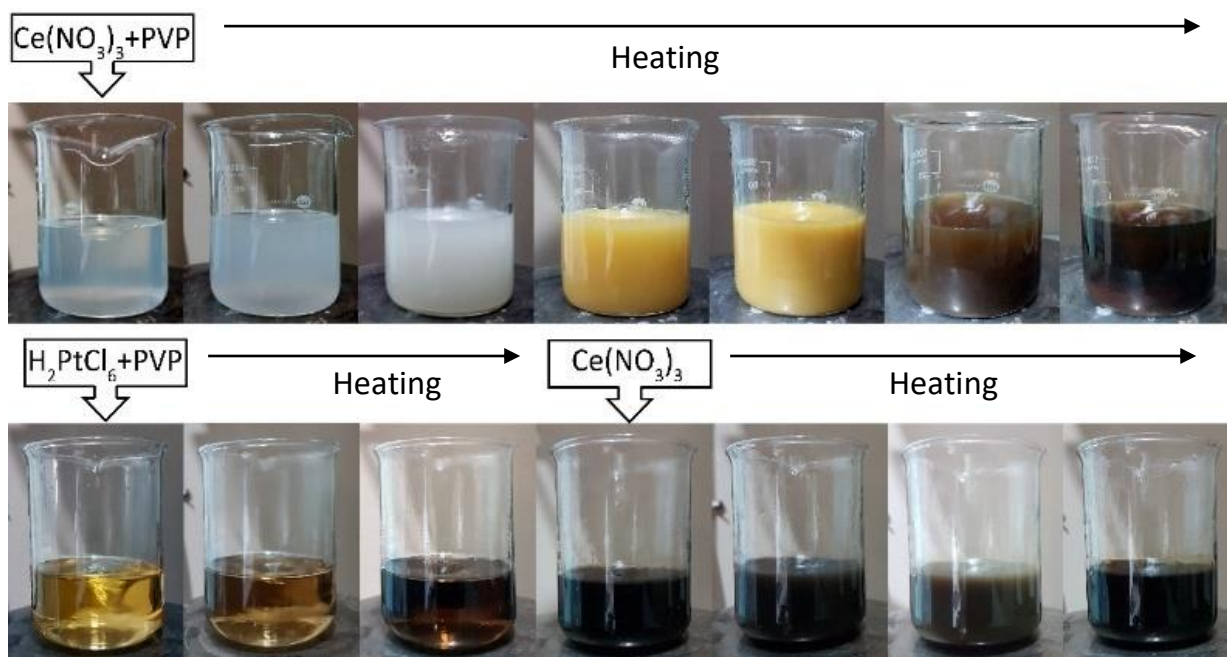
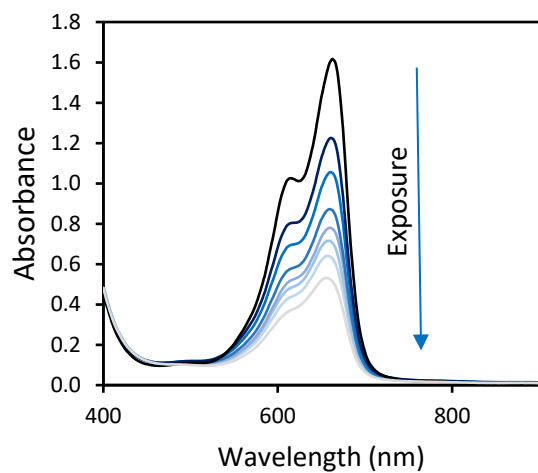
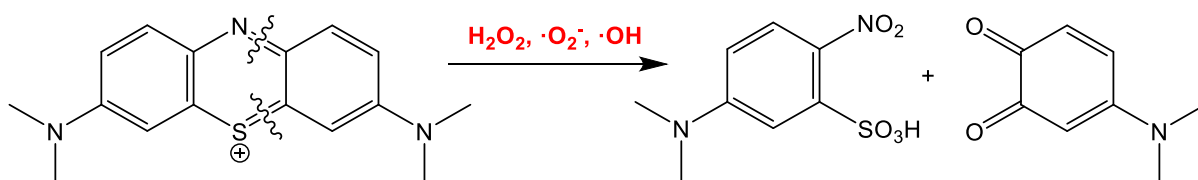


Fig. S1. Appearance of the systems during the synthesis: top – pristine  $\text{CeO}_2$  nanoparticles (PVP-CeNPs), bottom –  $\text{CeO}_2$  containing 2 wt.% of Pt nanoparticles (PVP-CeNPs-Pt). The preparation of pristine platinum nanoparticles (PVP-PtNPs) is the same as in the bottom figure before the addition of cerium salts.



Fenton mechanism and ROS formation:

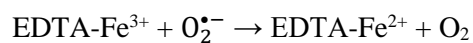
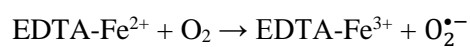
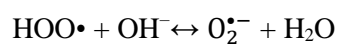


Fig. S2. (Top) Decomposition of MB and (bottom left) decrease of MB adsorption spectra under the Fenton reaction conditions at pH 7.0 in time (decrease of absorbance at  $\lambda_{\text{max}} = 662 \text{ nm}$ ). (Bottom right) The equation describing the Fenton mechanism and ROS formation.

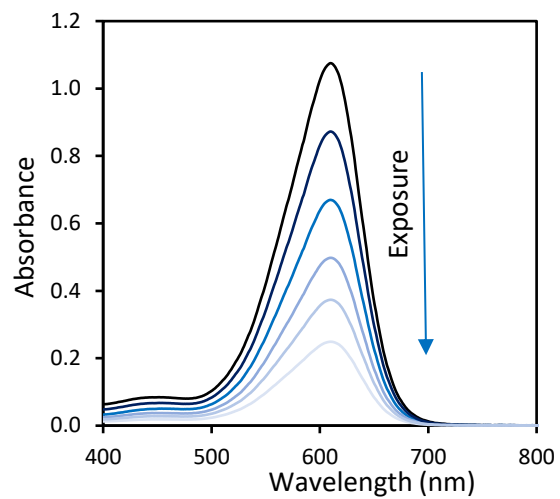
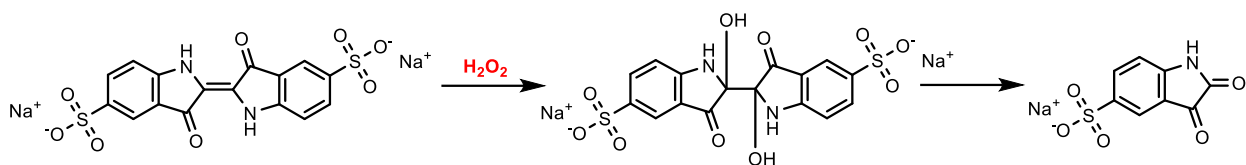


Fig. S3. (Top) Decomposition of IC and (bottom) decrease of IC adsorption spectra under the  $\text{H}_2\text{O}_2$  bleaching conditions at pH 7.0 in time (decrease of absorbance at  $\lambda_{\text{max}} = 610$  nm).

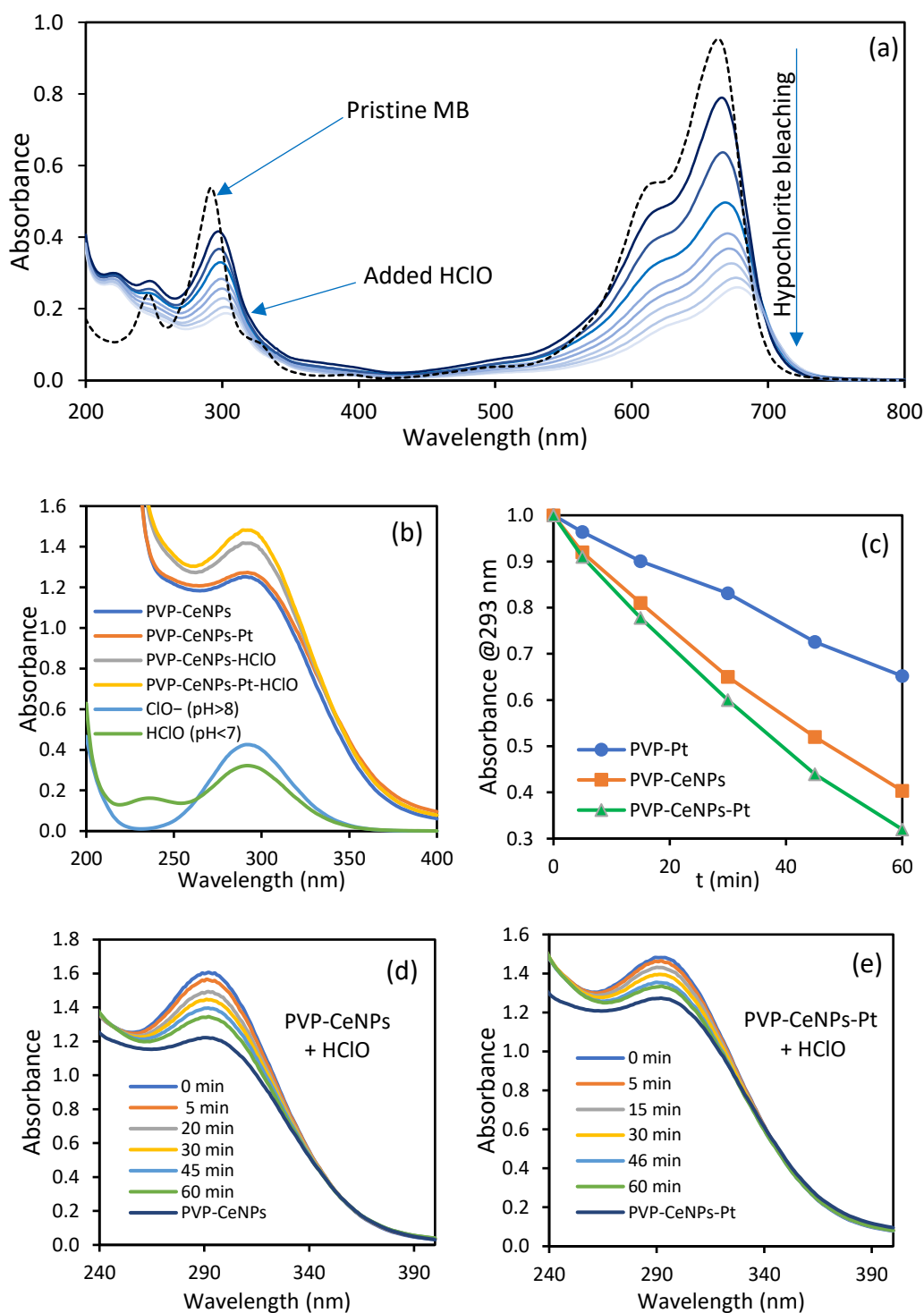


Fig. S4. (a) Decrease of MB adsorption spectra in the presence of HClO at pH 7.0 as a function of time. (b) Absorption spectra of PVP-CeNPs and PVP-CeNPs-Pt compared to spectra of PVP-CeNPs-HClO and PVP-CeNPs-Pt-HClO, and HClO and ClO<sup>-</sup> species at pH 7.0. (c) Dynamics of hypochlorite decomposition in the presence of PVP-CeNPs (~0.3 mM), PVP-CeNPs-Pt (~0.3 mM) and PVP-PtNPs (6 μM Pt) at pH 7.0 as a function of time. (d, e) The behavior of PVP-CeNPs-HClO and PVP-CeNPs-Pt-HClO adsorption spectra at pH 7.0 as a function of time.

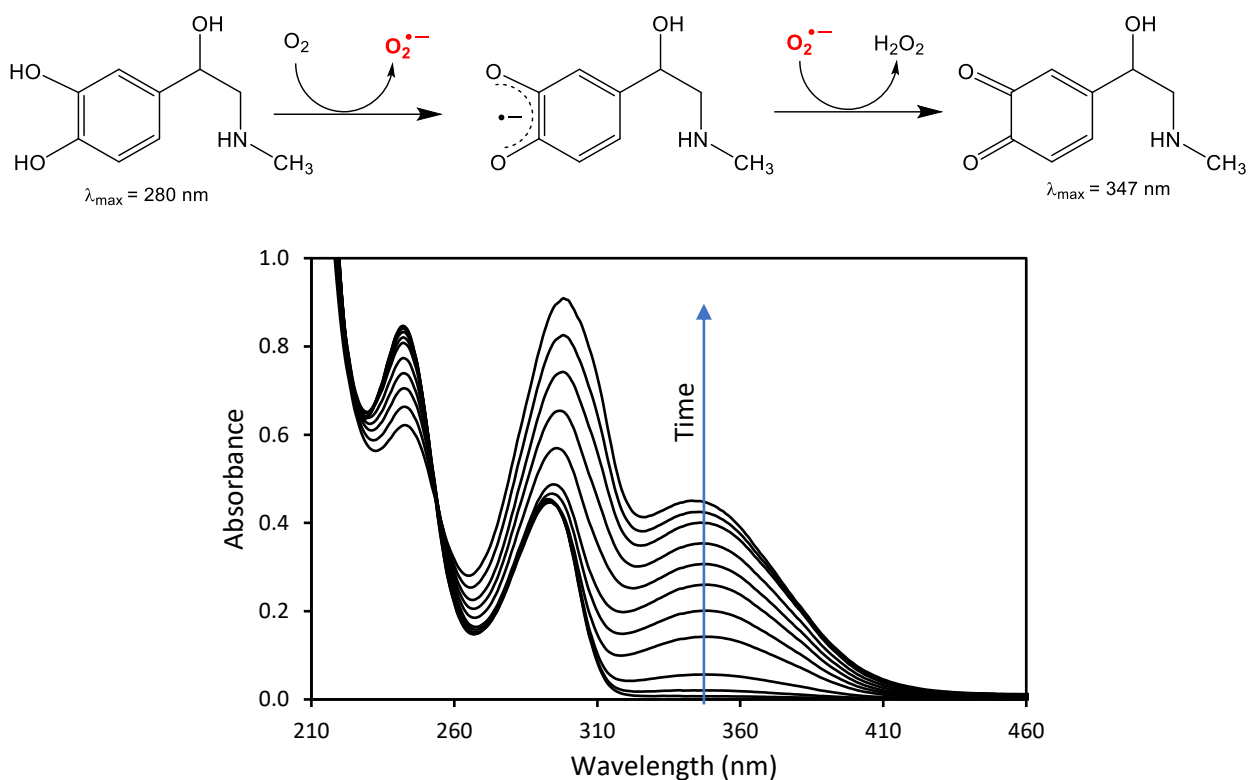


Fig. S5. (Top) Schematic of adrenaline autoxidation and (bottom) change of the absorption spectra as function of time (increase in absorbance at  $\lambda_{max} = 347$  nm).

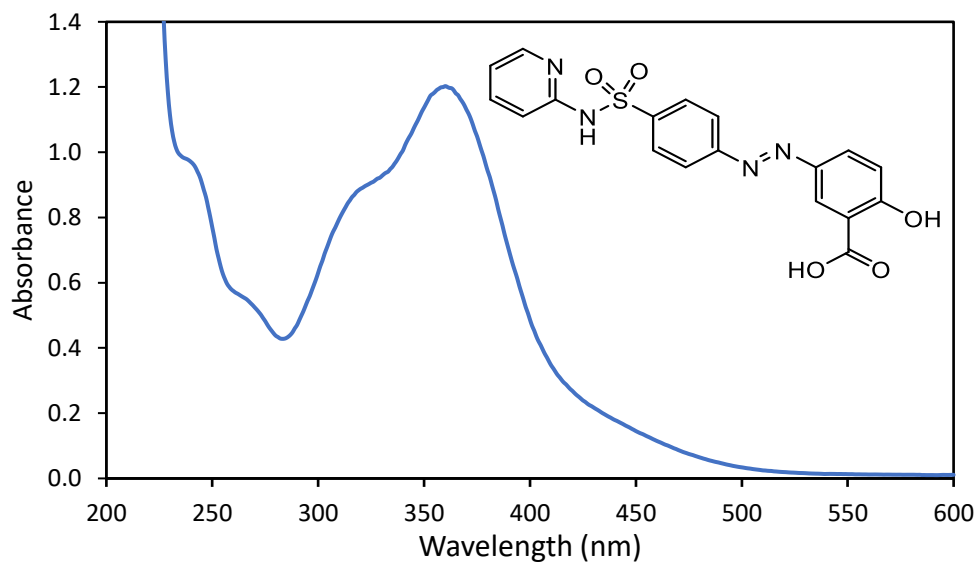


Fig. S6. UV-vis absorption spectrum of 0.1 mM sulfasalazine solution in water ( $\lambda_{max} = 360$  nm). The schematic structure of the sulfasalazine molecule is shown in the inset.